

JSACE 3/16

Improving Particle
Size Distribution
in Cement Paste
by Blending with
Superfine Cement

Received
2016/08/21

Accepted after
revision
2016/10/10

Improving Particle Size Distribution in Cement Paste by Blending with Superfine Cement

P.L. Ng

Department of Civil Engineering, The University of Hong Kong, Pokfulam, Hong Kong, China
Faculty of Civil Engineering, Vilnius Gediminas Technical University
Sauletekio Ave. 11, Vilnius LT-10223, Lithuania

J.J. Chen*

Department of Civil Engineering, Foshan University, 18 Jiangwan Road, Foshan, Guangdong, China

A.K.H. Kwan

Department of Civil Engineering, The University of Hong Kong, Pokfulam, Hong Kong, China

*Corresponding author: chenjjajian@fosu.edu.cn

 <http://dx.doi.org/10.5755/j01.sace.16.3.16273>

The rheological and mechanical performance of cement paste is closely related to its packing density, which may be optimized by improving the particle size distribution in the paste mix. In this study, the authors propose modifications to the existing mathematical equations of particle size distribution. The new equation of optimal particle size distribution so formulated is verified experimentally. A series of cement paste having different water/cementitious materials (W/CM) ratios were produced by blending ordinary Portland cement (OPC) with varying contents of superfine cement (SFC). The particle size distributions of the blended paste mixes were compared with the proposed equation. The packing density of paste mixes was measured using the wet packing test method, and the flowability, rheological properties, and compressive strength of the paste mixes were tested. It is found, that the particle size distribution in cement paste can be improved by blending with SFC, which can lead to enhancement in packing density, flowability, rheology and strength. The authors opine that the proposed equation of particle size distribution may be applied for mix design optimization of cementitious paste, including cementitious grout and the paste phase in mortar and concrete.

KEYWORDS: packing density, particle size distribution, paste, rheology, superfine cement.

Introduction



Cementitious paste is a mixture of water and cementitious materials. In a paste mix, the water must be sufficient to fill up the voids between solid ingredients, as any unfilled voids would become air voids and eventually porosity in the hardened paste (Kwan and Wong 2008). The rheological and mechanical performance of cementitious paste is closely related to its packing density. In fresh state, a high packing density would generally require less water to fill up the voids in the cementitious matrix. Therefore, for the same water/cementitious materials (W/CM) ratio, a greater amount of excess water (i.e. water in excess of that needed to fill the voids) would be available to lubricate the solid particles, thus improving the flowability and rheological performance. Alternatively, for the same flowability performance, the W/CM ratio may be reduced to improve the strength of hardened paste.

Theoretically, the packing density could be optimized by improving the particle size distribution in the paste mix. An optimal particle size distribution should be a continuous one such that the finer particles could fill into the voids between larger particles and reduce the overall volume of voids. This concept has been incorporated in devising mathematical equations of ideal particle size distributions for packing of aggregates for mortar and concrete (Andreasen and Andersen 1930, Furnas 1931). However, there has been a lack of well-proven particle size distribution model that could cater for the powder phase, which may be classified as finer than 75 μm in size. In fact, there is a common misunderstanding that the fines portion (which may be taken as in the size range of powder) in fine aggregate is always unfavourable to the quality of aggregate and hence the quality of mortar and concrete. In actual fact, the presence of appropriate proportions of fines can be beneficial to optimizing the packing density of fine aggregates (Kwan et al. 2014). Moreover, to improve the packing density of paste, the role of powders should be duly considered in the particle size distribution model.

As opposed to the continuous particle size distribution, in conventional cement concrete, the solid ingredients including cement grain, fine aggregate and coarse aggregate are not continuously graded. There are gaps in the size ranges of roughly 50 to 500 μm (lying between cement and fine aggregate) and smaller than 5 μm (finer than cement) (Chen 2012). These gaps may be filled by fillers of appropriate sizes. In connection to this, experimental investigations have demonstrated the positive role of fillers (including fines as part of fillers) in mortar and concrete (Chen et al. 2012). For conventional cement paste, there exists a gap in the size range of roughly 5 μm and below, which may be filled by appropriate fillers for improved particle size distributions in the paste. However, as pointed out in the above, due to a lack of established particle size distribution model to cater for the powder phase, the optimization of packing density of cementitious paste mix is usually performed by trial and error.

To enable optimizing the packing density of cementitious paste by a scientific approach, a new equation of optimal particle size distribution is developed herein. The equation is verified by an experimental programme encompassing a series of cementitious paste produced by blending ordinary Portland cement (OPC) and superfine cement (SFC) in different proportions. Details of the mathematical formulations and experimental investigations are reported hereunder.

The strategy of optimizing the particle size distribution to achieve maximum packing density had been adopted in the past for mortar and ceramic production. A number of ideal particle size distribution equations had been proposed. Early in the 30's in last century, Andreasen and Andersen (1930) put forward the below equation of ideal particle size distribution:

$$CPFT = \left(\frac{D}{D_L} \right)^m \times 100\% \quad (1)$$

where

CPFT is the "cumulative percentage finer than", *D* is the particle size, *D_L* is the largest particle size, and *m* is a distribution index or distribution modulus.

Equation (1) is commonly referred to as Andreasen's equation. It was validated experimentally by Andreasen and Andersen (1930), who suggested that the value of *m* should be between 0.33 and 0.50 for maximum packing density. By plotting *CPFT* against *D* with both axes drawn in logarithmic scale, the Andreasen's equation is represented by a straight line in the log-log plot.

Furnas (1931) and Anderegg (1931) investigated the packing of aggregates for mortar, and revised the mathematical formulation with consideration of the influence of smallest particle size on the particle size distribution. The ideal particle size distribution proposed by Furnas (1931) is given by:

$$CPFT = \left(\frac{r^h D - r^h D_s}{r^h D_L - r^h D_s} \right) \times 100\% \quad (2)$$

where

D_s is the smallest particle size, *r* is a distribution coefficient, and other symbols have the same meaning as in Equation (1).

Optimization of Particle Size Distribution

Funk and Dinger (1994) modified Andreasen's equation for applications in ceramic manufacturing. They advocated the strategy of predictive process control to maximize packing density by following the optimal particle size distribution (Dinger and Funk 1992, 1996, 1997, Dinger 2001, 2002). For this purpose, the below equation was proposed (Funk and Dinger 1994):

$$CPFT = \left(\frac{D^m - D_S^m}{D_L^m - D_S^m} \right) \times 100\% \quad (3)$$

Equation (3) is often referred to as modified Andreasen's equation. By means of numerical simulation, Funk and Dinger (1994) claimed that if the particles follow a continuous grading until down to an infinitely small particle size, then 100% packing

density (or 0% porosity) can be achieved when the distribution modulus m is smaller than or equal to 0.37. However, it is impossible to have infinitely small particles in reality. The role of smallest particle size D_S should be duly considered in the particle size distribution model. In this regard, the influence of D_S was ignored in Andreasen's equation but it was taken into account by Furnas (1931) and Funk and Dinger (1994).

Equations (1) to (3) above follow the principle of geometric similarity. In other words, if all the particles are enlarged or shrunk by the same ratio, the resulting packing density would remain unchanged. Besides, it can be shown mathematically that Equation (2) and Equation (3) are equivalent with the only difference of a constant of proportionality. In particular, if m is taken as $\ln(r)$, or r is taken as e^m , both equations would become identical.

Among various particle size distribution models, the modified Andreasen's equation has been applied to the production control of high-performance concrete (HPC) and yielded interim success (Zheng and Kwan 2006). In contrast to concrete and mortar, the aggregate phase is omitted in paste, while the powder phase in blended paste mixes exerts substantial influence on the packing of solids. As such, alterations to the particle size distribution model would be necessitated. Herein, the authors propose modifications to the existing mathematical equations. The new equation is given by Equation (4), in which p and q are modified distribution moduli, ζ is a dimensionless parameter as defined in Equation (5), and other symbols have the same meaning as previously defined.

$$CPFT = \left[\zeta \left(\frac{D^p - D_S^p}{D_L^p - D_S^p} \right) + (1 - \zeta) \left(\frac{D^q - D_S^q}{D_L^q - D_S^q} \right) \right] \times 100\% \quad (4)$$

$$\zeta = \left(\frac{\ln D - \ln D_S}{\ln D_L - \ln D_S} \right) \quad (5)$$

Experimental Verification

The proposed equation of optimal particle size distribution is experimentally verified with cementitious paste mixes produced from blending varying contents of ordinary Portland cement (OPC) and superfine cement (SFC). The experimental programme is described below. The OPC was of strength class 52.5N complying with European Standard EN 197-1: 2011. The SFC was produced in France and it contained 80% slag. The solid densities of the OPC and SFC were measured to be 3112 kg/m³ and 2940 kg/m³, respectively. With the use of laser diffraction particle size analyzer, the particle size distributions of OPC and SFC were measured as plotted in Fig. 1. Based on the particle size distributions so obtained, the mean particle sizes of OPC and SFC were evaluated respectively to be 12.4 μm and 3.1 μm, whereas their specific surface areas were evaluated respectively to be 1.014 × 10⁶ m²/m³ (equivalent to 326 m²/kg) and 2.293 × 10⁶ m²/m³ (equivalent to 780 m²/kg).

A polycarboxylate ether-based superplasticizer (SP) was added to the paste mixes for better dispersion of the cement. The SP was in aqueous solution state with solid mass content of 20% and

relative density of 1.03. In view of the large specific surface area of SFC, the saturation dosage of SP (which is a surface reactant) was more appropriately expressed in term of liquid mass per solid surface area of cementitious materials (kg/m^2). From previous studies, the saturation dosage of SP was found to be $26 \times 10^{-6} \text{ kg}/\text{m}^2$ (Kwan et al. 2012), this dosage was adopted for all cementitious paste mixes. It should be noted that if the dosage is converted to mass of SP per mass of cementitious materials, it would increase with the SFC content due to the high fineness of SFC relative to OPC.

In the following, the particle size distributions and packing densities of blended cementitious paste mixes are studied. The mixes were assigned the labels PD-0, PD-10, PD-20 and PD-30 with the SFC content varied amongst 0%, 10%, 20% and 30% by mass of the total cementitious materials, respectively. To determine the particle size distribution of the cementitious paste, the SFC content by mass needs to be converted to SFC content by volume using the below equation:

$$\frac{V_{SFC}}{V_{CM}} = \frac{\frac{(M_{SFC}/M_{CM}) \rho_{SFC}}{1 - (M_{SFC}/M_{CM}) + (M_{SFC}/M_{CM})}}{\rho_{OPC}} \quad (6)$$

In Equation (6), the subscript *CM* stands for cementitious materials (i.e. OPC together with SFC in this context), (V_{SFC}/V_{CM}) is the SFC content by volume, (M_{SFC}/M_{CM}) is the SFC content by mass, ρ_{SFC} is the

solid density of SFC, and ρ_{OPC} is the solid density of OPC.

With the SFC content by volume evaluated, the particle size distribution curves of PD-0, PD-10, PD-20 and PD-30 are determined as depicted in Fig. 2. The value of D_s in Equations (4) and (5) is taken as the size where no more than 2.0% of the particles by volume were finer, and it is found to be $1.0 \mu\text{m}$. The value of D_L in Equations (4) and (5) is taken as the size where no less than 98.0% of the particles by volume were coarser, and it is found to be $36.2 \mu\text{m}$. By numerical optimization, setting $q = -p = 0.16$ for the modified distribution moduli could best resemble the geometrical shape of particle size distribution curves of the blended cementitious paste. Correspondingly, the variation of *CPFT* with particle size *D* is evaluated as plotted in Fig. 2, and this represents the optimal particle size distribution.

From Fig. 2, it can be observed, that the particle size distribution of mix PD-0 (cement paste) does not resemble the curve of optimal particle size distribution. By blending with SFC, the particle size distributions of PD-10 and PD-20 are close to the optimal curve, this indicates the desirable effect of SFC in improving the particle size distribution. However, when the SFC content is further increased, the particle size distribution of PD-30 becomes dissimilar to the optimal curve. It is because the SFC content of 30% is excessive.

For ease of visualizing the effect of values of *p* on the shape of particle size distribution curve,

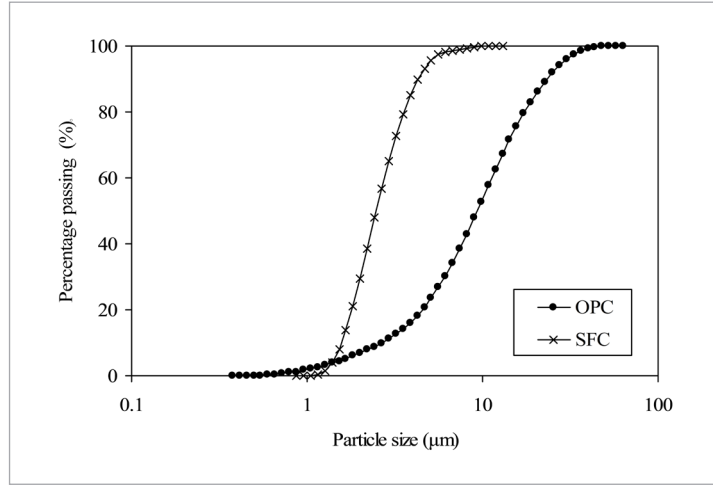


Fig. 1 Particle size distributions of OPC and SFC

Fig. 2

Particle size distributions of cementitious paste

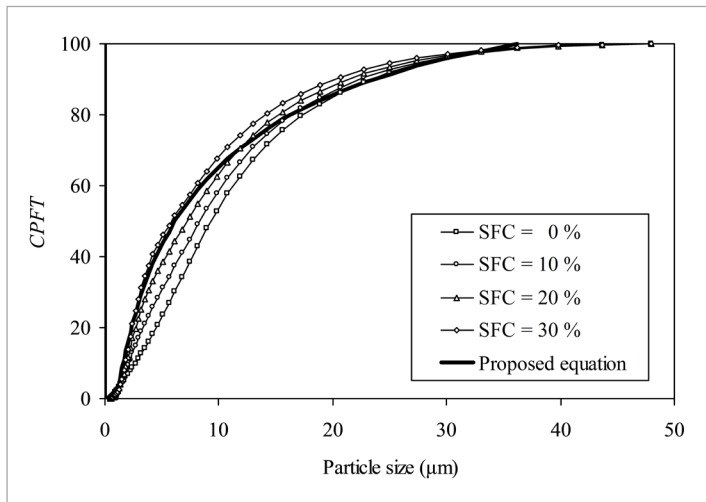


Fig. 3

Particle size distribution curves per modified Andreasen's equation and proposed model

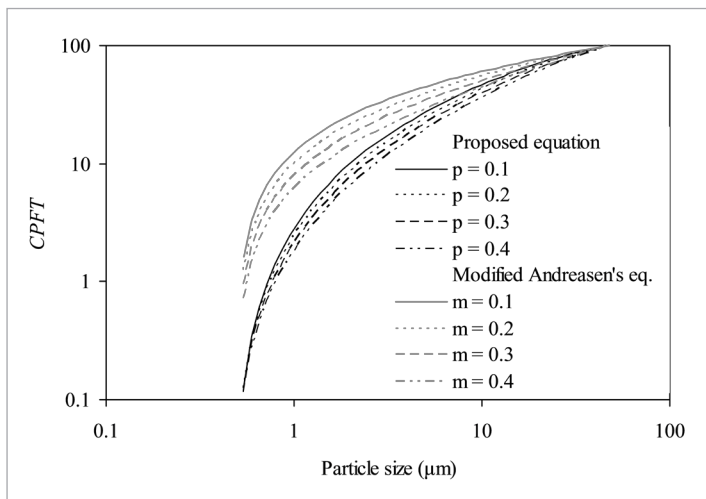


Fig. 3 plots the variations of *CPFT* with *D* calculated per Equation (4) for $p = 0.1, 0.2, 0.3$ and 0.4 . The value of q is fixed at 1.0 for comparison with the modified Andreasen's equation. In general, the smaller is the value of p , the higher is the curve of *CPFT*. In other words, a smaller value of modified distribution modulus indicates higher content of finer particles and vice versa. In contrast, from previous studies on production of HPC (Zheng and Kwan 2006), it had been concluded that for HPC mixes with desirable flowability and strength performance, the values of distribution modulus m were within the range from 0.22 to 0.26 in the modified Andreasen's equation (Funk and Dinger 1994). The *CPFT* calculated per Equation (3) with the values of m varying from 0.1 to 0.4 are plotted in Fig. 3.

The packing densities of cementitious paste mixes were measured using the wet packing test method. The procedures of wet packing test have been outlined in Wong et al. (2007) and Wong and Kwan (2008a). The principle behind the wet packing test is briefly explained as follows. The solid concentration ϕ refers to the ratio of solid volume of cementitious materials V_{CM} to the bulk volume of paste mix V , i.e.:

$$\phi = V_{CM}/V \tag{7}$$

The voids content ε is defined as the ratio of volume of voids to the bulk volume of paste mix, and the voids ratio u is defined as the ratio

of volume of voids to the solid volume of cementitious materials. Therefore,

$$\varepsilon = (V - V_{CM})/V \tag{8}$$

$$u = \frac{\varepsilon}{1 - \varepsilon} \tag{9}$$

The subjects of Equations (7) to (9) are inter-related by the following equation:

$$\phi = 1 - \varepsilon = \frac{1}{1 + u} \tag{10}$$

Mix no.	SFC content (%)	Packing density	Change in packing density (%)	Voids ratio	Change in voids ratio (%)
PD-0	0%	0.637	-	0.570	-
PD-10	10%	0.659	+3.4%	0.517	-9.3%
PD-20	20%	0.679	+6.6%	0.473	-17.0%
PD-30	30%	0.678	+6.4%	0.475	-16.7%

Table 1

Packing density and voids ratio of cementitious paste mixes

For a paste mix with a given proportioning of cementitious materials, ϕ and u are dependent on the W/CM ratio. Generally, as the W/CM ratio increases from an inadequately low value, ϕ increases with water content until attaining the maximum, and then decreases with further increasing water content. The maximum solid concentration ϕ_{max} corresponds to the minimum voids ratio u_{min} .

For ease of reference, the paste mixes for packing density measurement are assigned mix numbers in the form of PD-(SFC content). For each of the mixes PD-0, PD-10, PD-20 and PD-30 as given in Table 1, multiple samples of cementitious materials in the same proportioning were each mixed with water at varying W/CM ratio and with the same dosage of SP. The bulk density of each sample was measured and the maximum solid concentration ϕ_{max} amongst the samples was determined as the packing density. Table 1 lists the packing density and voids ratio results. Comparing the paste mixes with and without SFC, the positive effects of blending with SFC as demonstrated by the increase in packing density and reduction in voids ratio are apparent. However, when the SFC content increased from 20% to 30%, the packing density decreased slightly and the voids ratio increased slightly. Using the mix PD-0 as the baseline of comparison, the maximum increase in packing density was 6.6% at SFC content of 20%, and the corresponding reduction in voids ratio was 17.0%.

In the next step, the flow spread, flow rate, rheological properties and cube strength of cementitious paste mixes with various SFC contents and W/CM ratios were evaluated. This is for the purpose of verifying the positive effects of improved particle size distribution on the performance of cementitious paste. As shown earlier, the particle size distribution and packing density of cementitious paste blended with 30% SFC are not desirable. Hence, such a high SFC content was not adopted. In the remaining investigations of flowability, rheology and strength, the SFC content by mass was varied among 0, 10% and 20%. The W/CM ratio by mass was varied from 0.18 to 0.30 in increments of 0.02. For ease of reference, each of the cementitious paste mixes is assigned a number in the form of CP-(SFC content)-(W/CM ratio).

Due to the high fineness of SFC, during mixing with water, the cementitious materials would tend to form water-bound granules with dry surfaces rather than coalesced to become a thick paste, even if the mixing time is reasonably prolonged. To facilitate thorough mixing of the ingredients, a special mixing sequence such that the cementitious materials and SP were divided into several portions, which were added one at a time to the water in the mixing bowl and mixed to form a slurry (Wong and Kwan 2008a), was required.

The flow spread represents the static flowability of cementitious paste, and it was measured with the mini slump cone test. Details of the mini slump cone have been described in Okamura and Ouchi (2003). The flow rate represents the dynamic flowability of cementitious paste, and it was measured with the Marsh cone test as specified in European Standard EN 445: 2007. The rheological properties were obtained using a shear rate-controlled rheometer (Fig. 4) which applied

Fig. 4

Rheometer employed
in study



torque through the spindle to shear the paste sample. The shearing sequence was applied in two cycles: the first shearing cycle (pre-shearing cycle) for ensuring each paste sample had undergone the same shearing history before measurement; and the second shearing cycle (data-logging cycle) for actual measurement and recording by a data-logger (Wong and Kwan 2008b). During each shearing cycle, the shear rate was increased from 0 to 50 s⁻¹ in 75 sec, and then decreased to 0 s⁻¹ in another 75 sec. Two shear stress (τ) versus shear rate ($\dot{\gamma}$) curves, one at increasing shear rate and the other at decreasing shear rate, could be obtained. The latter τ - $\dot{\gamma}$ curve, which was generally more consistent and repeatable, was used for evaluating the rheological properties of the paste sample. Finally, the compressive strength was obtained from cube crushing test with 70.7 mm cubes based on averaged results of 3 cubes.

Rheological and Mechanical Performance of Paste

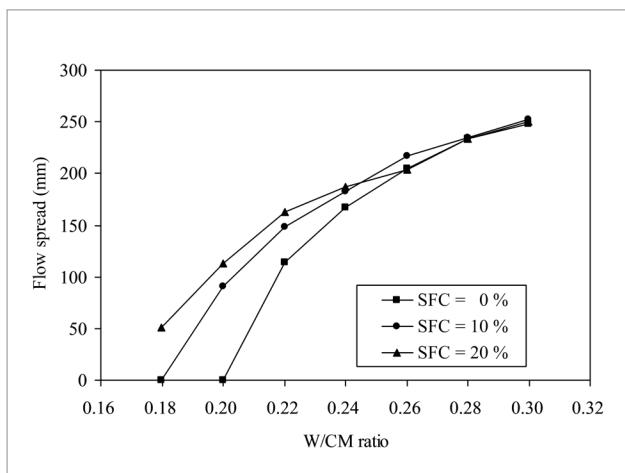
The flow spread and flow rate results are summarized in Table 2. The flow spread is plotted against the W/CM ratio in Fig. 5, from which it can be seen that by blending with SFC in the paste mixes, the flow spread-W/CM curve was shifted upwards and to the left. In other words, the flow spread is increased at the same W/CM ratio, and for the same flow spread performance a lower W/CM can be adopted to achieve higher strength and denser microstructure. Besides, it is observed that when the W/CM ratio is lower than 0.24, the flow spread-W/CM curve for 20% SFC content lies above the curve for 10% SFC, indicating better flowability of paste samples with 20% SFC. Nevertheless, the two curves intersect at W/CM ratio of around 0.24 and at higher W/CM ratios, the flow spread of paste samples with 10% SFC was marginally larger than that of paste samples with 20% SFC.

The results of flow rate demonstrate similar trend to the flow spread. With addition of SFC, a higher flow rate than cement paste without SFC could be obtained. Moreover, blending with 20% SFC is more beneficial than blending with 10% SFC when the W/CM ratio is lower than 0.26. Nev-

ertheless, when the W/CM ratio is at 0.26 or higher, the flow rates of paste samples with SFC contents of 10% and 20% are similar. At W/CM ratio equal to 0.30, the flow rate of paste sample with 10% SFC is higher than that of paste sample with 20% SFC. The flow rate is plotted against the flow spread in Fig. 6. It is obvious that the flow spread and flow rate are highly correlated, regardless of the SFC content. Therefore, it can be concluded that the static flowability and dynamic flowability of

Fig. 5

Flow spread versus W/
CM ratio



Mix no.	Flow spread (mm)	Flow rate (ml/s)	Yield stress (Pa)	Apparent viscosity (Pa-s)	Flow index	7-day cube strength (MPa)	28-day cube strength (MPa)	Ratio of 28-day strength to 7-day strength
CP-0-0.18	0.0	0.0	-	-	-	93.7	97.7	1.04
CP-0-0.20	0.0	0.0	-	-	-	95.4	105.7	1.11
CP-0-0.22	113.5	2.1	17.53	3.23	1.16	108.1	119.4	1.10
CP-0-0.24	167.0	7.4	6.66	1.98	1.23	105.5	119.1	1.13
CP-0-0.26	205.0	9.9	3.89	1.47	1.32	101.5	116.4	1.15
CP-0-0.28	233.3	13.2	2.01	1.05	1.34	94.7	104.7	1.11
CP-0-0.30	248.5	15.5	0.96	0.79	1.39	87.1	98.6	1.13
CP-10-0.18	0.0	0.0	-	-	-	108.5	113.7	1.05
CP-10-0.20	90.8	1.1	29.86	4.39	1.07	116.9	119.8	1.02
CP-10-0.22	148.3	4.1	10.62	2.73	1.12	115.4	124.8	1.08
CP-10-0.24	183.0	8.1	8.23	1.86	1.21	112.8	122.9	1.09
CP-10-0.26	217.0	10.8	3.12	1.41	1.29	104.6	117.1	1.12
CP-10-0.28	234.5	13.6	2.02	1.08	1.35	101.7	110.9	1.09
CP-10-0.30	252.0	17.0	1.05	0.71	1.41	94.5	102.3	1.08
CP-20-0.18	51.0	0.0	-	-	-	126.2	130.3	1.03
CP-20-0.20	112.8	2.0	33.43	5.03	1.01	136.7	137.7	1.01
CP-20-0.22	163.0	5.7	16.81	3.10	1.05	131.0	132.1	1.01
CP-20-0.24	186.8	9.3	12.73	2.06	1.16	123.1	129.5	1.05
CP-20-0.26	204.0	11.1	6.37	1.71	1.22	113.4	121.9	1.07
CP-20-0.28	233.8	13.8	2.97	1.46	1.31	105.7	116.4	1.10
CP-20-0.30	250.3	16.2	2.63	0.90	1.38	99.8	104.2	1.04

Table 2

Experimental results of cementitious paste mixes

the cementitious paste correlate strongly with each other.

From the rheometer testing, the shear stress-shear rate curve obtained may be described in terms of an appropriate rheological model, such as the commonly used Bingham model (Bingham 1916) and Herschel-Bulkley model (Herschel and Bulkley 1926). The Bingham model is given by the following equation:

$$\tau = \tau_y + \mu\dot{\gamma} \quad (11)$$

$$\tau = \tau_y + K\dot{\gamma}^n \quad (12)$$

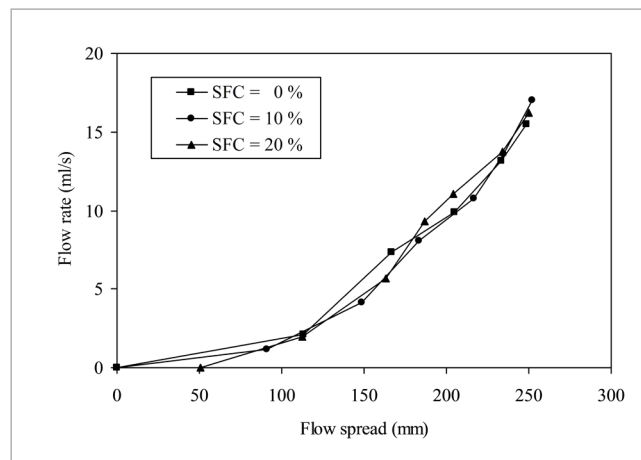


Fig. 6

Flow rate versus flow spread

where τ (Pa) is the shear stress, τ_y (Pa) is the yield stress, $\dot{\gamma}$ (s^{-1}) is the shear rate, and μ (Pa-s) is the plastic viscosity. The Herschel-Bulkley model is given by the following equation:

where K ($Pa \cdot s^n$) is the consistency index, n (dimensionless) is the flow index, and other symbols have the same meaning as defined in Equation (11). It was found that the Her-

Fig. 7

Yield stress versus flow rate

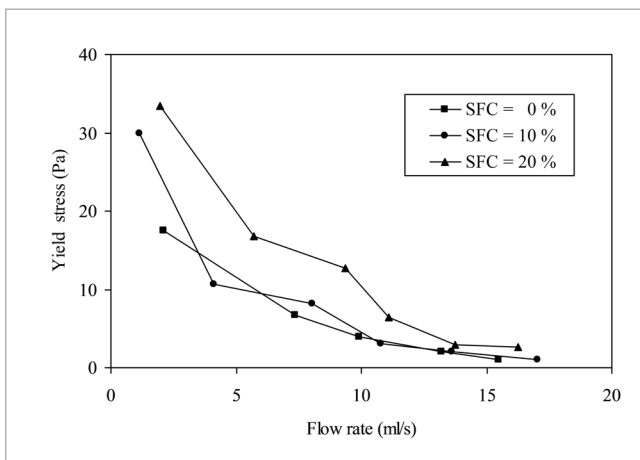


Fig. 8

Apparent viscosity versus flow rate

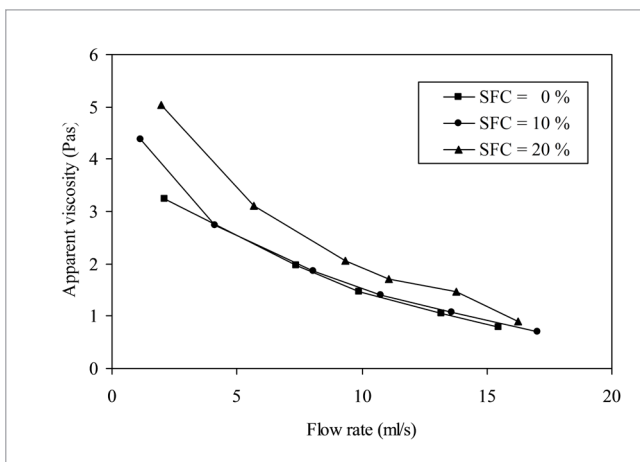
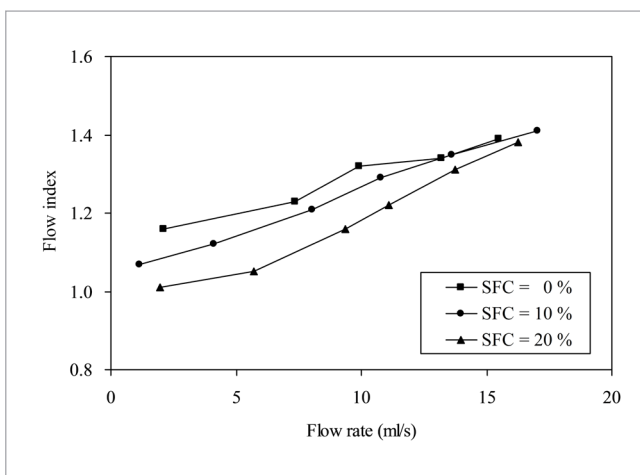


Fig. 9

Flow index versus flow rate



schel-Bulkley model agreed better with the experimental results and it was therefore adopted in evaluating the rheological properties of cementitious paste mixes. For each paste sample, the best-fit curve that accorded with Equation (12) was obtained by regression analysis. From the best-fit curve, τ_y is taken as the value of τ at $\dot{\gamma} = 0 \text{ s}^{-1}$, and the apparent viscosity μ_a (Pa·s) is taken as the ratio of $\tau/\dot{\gamma}$ at $\dot{\gamma} = 50 \text{ s}^{-1}$. The n -value of the best-fit curve represents the degree of shear thickening of the cementitious paste: if $n < 1$, it implies shear thinning, whereas if $n > 1$, it implies shear thickening. The values of τ_y , μ_a and n for the paste mixes are summarized in Table 2.

From the tabulated results, it can be seen that in general, τ_y and μ_a decreased with increasing W/CM, and n increased with increasing W/CM. The effects of 10% SFC content on τ_y and μ_a are not very pronounced, while at 20% SFC content, both τ_y and μ_a were increased. A higher SFC content caused n to decrease (i.e. the degree of shear thickening was reduced) when the W/CM ratio was lower than 0.28, while the effect of SFC content on n was insignificant when the W/CM ratio was higher than 0.28. On the other hand, the rheological properties are more related to the flow rate (which represents the dynamic flowability) of paste mixes, as shown below.

In Fig. 7 to Fig. 9, the τ_y , μ_a and n values are respectively plotted

against the flow rate. It can be seen in Fig. 7 that τ_y generally decreased with increasing flow rate. The yield stress-flow rate curves for paste with 0% and 10% SFC contents intersect at a number of points, while the curve for paste with 20% SFC content was shifted upwards, indicating a higher τ_y at the same level of flow rate. Similar observations are noted in Fig. 8, where μ_a generally decreased with increasing flow rate. The apparent viscosity-flow rate curves for paste with 0% and 10%

SFC contents overlap at a number of portions, while the curve for paste with 20% SFC content was shifted upwards, indicating a higher μ_o at the same flow rate. In Fig. 9, it can be seen that the flow index-flow rate curves were shifted downwards as the SFC content increased from 0% through 10% to 20%, indicating a smaller degree of shear thickening at the same level of flow rate.

The results of 7-day and 28-day cube compressive strength and the ratio of 28-day strength to 7-day strength are summarized in Table 2. The maximum 28-day compressive strength achieved by cement paste without SFC was 119.4 MPa, while that achieved by paste with 10% and 20% SFC contents was respectively 124.8 MPa and 137.7 MPa. The 28-day strength is plotted against the W/CM and against the flow spread in Fig. 10 and Fig. 11, respectively. It is evident from Fig. 10 that there existed a certain optimum W/CM ratio for maximum cube strength.

When the W/CM ratio was lower than the optimum value, the strength increased with the W/CM ratio, whilst when the W/CM ratio was higher than the optimum value, the strength decreased with increasing W/CM ratio. Moreover, it is observed that the optimum W/CM ratio decreased at higher SFC content. Therefore, blending with SFC would allow the adoption of a lower W/CM ratio to achieve higher strength.

Refer to Fig. 11, the concurrent strength-flowability performance of cementitious paste is inspected. Similar to the W/CM ratio, there is also certain optimum value of flow spread for maximum cube strength. As the SFC content increased from 0% through 10% to 20%, the strength-flowability performance curve was shifted upwards and to the right. This means by blending with SFC, both the strength and flowability of the cementitious paste can be increased simultaneously. The positive effects of SFC on concurrent strength-flowability performance would be attributed to the improvement of particle size distribution in the paste mix.

The ratio of 28-day strength to 7-day strength is plotted against the flow spread in Fig. 12. Amongst all mixes, the ratio ranged from 1.02 to 1.15. In other words, at the age of 7 days, the paste mixes developed 87% to 99% of the 28-day strength. The curves in Fig. 12 manifested a downward-shifting trend as the SFC content increased from 0% through 10% to 20%. This may be explained by the larger specific surface area of SFC to facilitate chemical reactions and enhance early-age strength development.

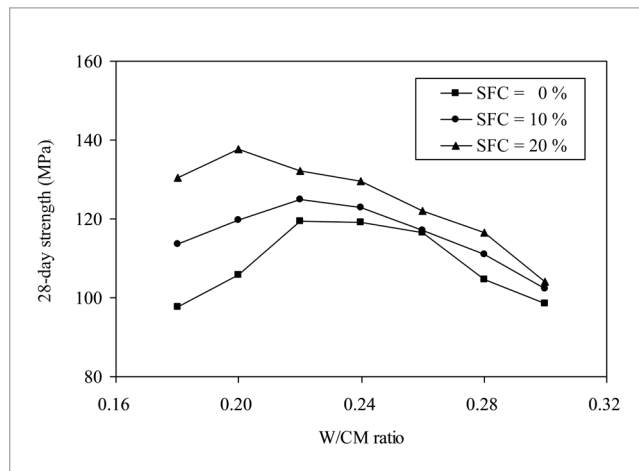


Fig. 10

Compressive strength versus W/CM

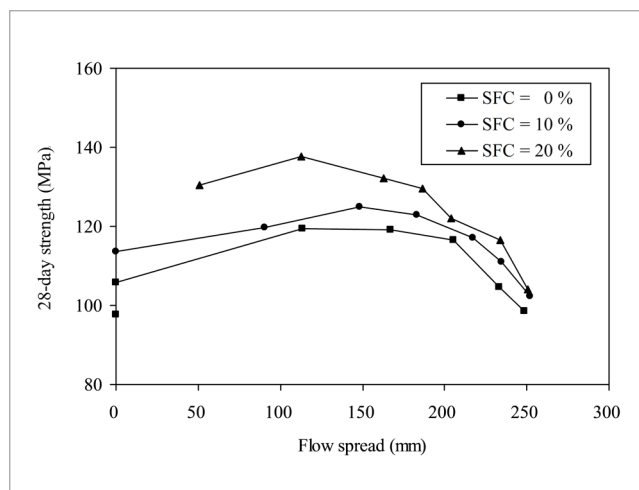
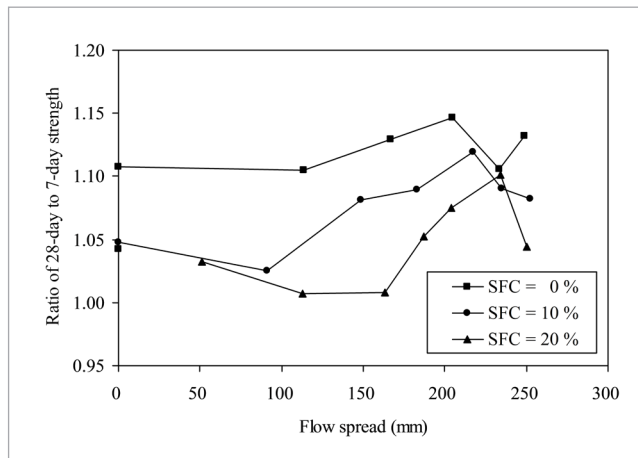


Fig. 11

Compressive strength versus flow spread

Fig. 12

Ratio of 28-day strength to 7-day strength versus flow spread



The above experimental results demonstrated the beneficial effects of blending with SFC on the packing density, rheological and mechanical properties of cementitious paste. Overall, in terms of packing density, flowability and strength, the paste samples blended with 20% SFC would outperform paste samples blended with 10% SFC, except the flow spread and flow rate of paste samples with 10% SFC at relatively high W/CM ratio were larger than or similar to

those of paste samples with 20% SFC. In terms of yield stress and apparent viscosity, the paste samples blended with 10% SFC would be lower than those of paste samples with 20% SFC. The yield stress and viscosity should not be excessive and their desired ranges would be dependent on applications. For example, to achieve self-levelling property for high-flowability mortar, accessibility to far-reaching corners and passing ability through obstructions for self-consolidating concrete, and penetrability into gaps and fissures for cementitious grout, the yield stress and viscosity should be limited. The beneficial effects of blending with SFC would be due to the improvement in particle size distribution, which becomes closer to the proposed optimal curve. Further experimental verifications with additional paste mixes containing various types of supplementary cementitious materials and fillers are necessary, in order to confirm the accuracy and universal applicability of the equation of optimal particle size distribution. Moreover, further research is needed to generalise the proposed equation to aid the mix design of mortar and concrete.

Conclusions

The existing mathematical models of ideal particle size distribution, which originated from aggregates for mortar and have been applied to mortar and concrete production, did not cater for the powder phase and hence is not directly applicable to cementitious paste mixes where the powder phase plays an important role while the aggregate phase is absent. Modifications to the existing equations are necessary. A new equation of optimal particle size distribution has been developed in this paper. The proposed equation has been verified experimentally based on cementitious paste mixes produced by blending superfine cement (SFC) with ordinary Portland cement (OPC). The particle size distribution of cementitious paste blended with SFC was shown to be closer to the optimal particle size distribution. The wet packing density, flowability, rheology and strength performance of the cementitious paste mixes were measured. Experimental results have demonstrated improvement in properties by blending with SFC, which rendered the particle size distribution in cementitious paste closer to the optimal. Subject to further investigations to confirm its accuracy, the authors advocate utilization of the proposed equation of optimal particle size distribution for mix design optimization of cementitious paste, including cementitious grout and the paste phase in mortar and concrete. Further research is needed to generalise the proposed equation to aid the mix design of mortar and concrete.

Acknowledgment

The second author acknowledges the financial supported by the PhD Start-up Fund of Natural Science Foundation of Guangdong Province, China (Project No. 2014A030310273).

Anderegg F.O. Grading aggregates II: the application of mathematical formulas to mortars. *Industrial and Engineering Chemistry*, 1931; 23(9): 1058-1064. <https://doi.org/10.1021/ie50261a018>

Andreasen A.H.M., Andersen J. Ueber die beziehung zwischen kornabstufung und zwischenraum in produkten aus losen körnern (mit einigen experimenten). *Kolloid-Zeitschrift*, 1930; 50(3): 217-228. <https://doi.org/10.1007/BF01422986>

Bingham E.C. An investigation of the laws of plastic flow. *Bulletin of the Bureau of Standards*, 1916; 13: 309-353. <https://doi.org/10.6028/bulletin.304>

Chen J.J. Use of Fillers to Improve Packing Density and Performance of Concrete. PhD Thesis, The University of Hong Kong; 2012.

Chen J.J., Fung W.W.S., Ng P.L., Kwan A.K.H. Adding fillers to reduce embodied carbon and embodied energy of concrete. In: *Proceedings, Twelfth International Conference on Recent Advances in Concrete Technology and Sustainability Issues*, Prague, Czech Republic; 2012: 91-107.

Dinger D.R. Particle Calculations for Ceramists. Clemson, South Carolina: Dinger Ceramic Consulting Services; 2001.

Dinger D.R. Rheology for Ceramists. Clemson, South Carolina: Dinger Ceramic Consulting Services; 2002.

Dinger D.R., Funk J.E. Predictive process control - computer programs for fine particle processing controls. *Ceramic Engineering & Science Proceedings*, 1992; 13(1-2): 296-309.

Dinger D.R., Funk J.E. Predictive process control: varying raw materials properties can produce constant body properties. *Ceramic Engineering & Science Proceedings*, 1996; 17(1): 72-76. <https://doi.org/10.1002/9780470314807.ch12>

Dinger D.R., Funk J.E. Particle packing phenomena and their application in materials processing. *MRS Bulletin*, 1997; 22(12): 19-23. <https://doi.org/10.1557/S0883769400034692>

Furnas C.C. Grading aggregates I - mathematical relations for beds of broken solids of maximum density. *Industrial and Engineering Chemistry*, 1931; 23(9): 1052-1058. <https://doi.org/10.1021/ie50261a017>

Funk J.E., Dinger D.R. Predictive Process Control of Crowded Particulate Suspensions: Ap-

plied to Ceramic Manufacturing. Dordrecht, The Netherlands: Kluwer Academic Publishers; 1994. <https://doi.org/10.1007/978-1-4615-3118-0>

Herschel W.H., Bulkley R. Konsistenzmessungen von gummi-benzollösungen. *Kolloid-Zeitschrift*, 1926; 39(4): 291-300. <https://doi.org/10.1007/BF01432034>

Kwan A.K.H., Chen J.J., Fung W.W.S. Effects of superplasticiser on rheology and cohesiveness of CSF cement paste. *Advances in Cement Research*, 2012; 24(3): 125-137. <https://doi.org/10.1680/adcr.10.00020>

Kwan A.K.H., Ng P.L., Huen K.Y. Effects of fines content on packing density of fine aggregate in concrete. *Construction and Building Materials*, 2014; 61: 270-277. <https://doi.org/10.1016/j.conbuildmat.2014.03.022>

Kwan A.K.H., Wong H.H.C. Effects of packing density, excess water and solid surface area on flowability of cement paste. *Advances in Cement Research*, 2008; 20(1): 1-11. <https://doi.org/10.1680/adcr.2008.20.1.1>

Okamura, H., Ouchi, M. Self-compacting concrete. *Journal of Advanced Concrete Technology*, 2003; 1(1): 5-15. <https://doi.org/10.3151/jact.1.5>

Wong H.H.C., Kwan A.K.H. Packing density of cementitious materials: measurement and modelling. *Magazine of Concrete Research*, 2008a; 60(3): 165-175. <https://doi.org/10.1680/mac.2007.00004>

Wong H.H.C., Kwan A.K.H. Rheology of cement paste: role of excess water to solid surface area ratio. *Journal of Materials in Civil Engineering*, 2008b; 20(2): 189-197. [https://doi.org/10.1061/\(ASCE\)0899-1561\(2008\)20:2\(189\)](https://doi.org/10.1061/(ASCE)0899-1561(2008)20:2(189))

Wong H.H.C., Ng I.Y.T., Ng P.L., Kwan A.K.H. Increasing packing density through ternary blending cement, fly ash and silica fume to improve cement paste rheology. In: *Malhotra V.M. Fly Ash, Silica Fume, Slag, and Natural Pozzolans in Concrete*, ACI Special Publication SP-242. Michigan: American Concrete Institute; 2007: 433-446.

Zheng W., Kwan A.K.H. Optimising packing density for production of flowing high-performance concrete. In: *Proceedings, International Conference on Bridge Engineering - Challenges in the 21st Century*, Hong Kong; 2006.

References

About the authors

PUI-LAM NG

Researcher

Department of Civil Engineering,
The University of Hong Kong

Adjunct professor

Faculty of Civil Engineering,
Vilnius Gediminas Technical
University

Main research area

Sustainable concrete materials
and structures, high-performance
cementitious composites

Address

Sauletekio Al. 11, Vilnius LT-
10223, Lithuania
Tel. +852-95875310 /
+370- 62423921
E-mail: irdngpl@gmail.com

JIAJIAN CHEN

Lecturer

Department of Civil
Engineering, Foshan University

Main research area

High-performance concrete
and mortar, concrete
technology

Address

18 Jiangwan Road, Foshan,
Guangdong Province, China
Tel. +86-13450891042
E-mail: chenjiajian@fosu.edu.
cn

ALBERT KWOK-HUNG KWAN

Professor

Department of Civil Engineering, The
University of Hong Kong

Main research area

Tall buildings, crack control of
concrete structures, concrete
materials and science

Address

Pokfulam, Hong Kong SAR, China
Tel. +852-28592647
E-mail: khkwan@hku.hk